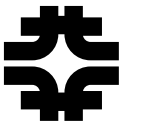

Fermilab

FERMILAB-PUB-06-516

Development of a Same-Side Kaon Tagging Algorithm of B_s^0 Decays for Measuring Δm_s at CDF II

Stephanie Menzemer
Ruprecht-Karls-Universität Heidelberg

We developed a Same-Side Kaon Tagging algorithm to determine the production flavor of B_s^0 mesons. Until the B_s^0 mixing frequency is clearly observed the performance of the Same-Side Kaon Tagging algorithm can not be measured on data but has to be determined on Monte Carlo simulation. Data and Monte Carlo agreement has been evaluated for both the B_s^0 and the high statistics B^+ and B^0 modes. Extensive systematic studies were performed to quantify potential discrepancies between data and Monte Carlo. The final optimized tagging algorithm exploits the particle identification capability of the CDF II detector. It achieves a tagging performance of $\epsilon D^2 = 4.0^{+0.9}_{-1.2}$ % on the $B_s^0 \to D_s^- \pi^+$ sample. The Same-Side Kaon Tagging algorithm presented here has been applied to the ongoing B_s^0 mixing analysis, and has provided a factor of 3-4 increase in the effective statistical size of the sample. This improvement resulted in the first direct measurement of the B_s^0 mixing frequency.

I. INTRODUCTION

The heavy and light mass eigenstates of neutral B mesons do not correspond to their weak interaction eigenstates. Therefore neutral B mesons are known to mix, where the mixing frequency Δm is the mass difference of the heavy and light mass eigenstate. While the mixing frequency (Δm_d) of $B^0 - \bar{B^0}$ oscillation has been precisely measured, the fast B_s^0 mixing frequency Δm_s has not yet been resolved. Combined direct measurements placed a lower bound of $\Delta m_s > 14.5$ ps^{-1} [1], while indirect measurements predict $\Delta m_s < 24$ ps^{-1} within the Standard Model [2]. The mixing frequencies Δm_d and Δm_s are related to fundamental Standard Model parameters which are not very well determined so far. Uncertainties to theoretical input almost cancel by studying the ratio $\frac{\Delta m_s}{\Delta m_d}$. Thus the precision measurement of Δm_s is a very important test of the Standard Model.
A mixing analysis consist of several steps. First the B_s^0 candidates are reconstructed. Then the proper time of the B_s^0 candidate is measured. An excellent proper time resolution is crucial to resolve the fast B_s^0 oscillations. Next we need to determine whether the B_s^0 candidate has mixed or not between production and decay. The decay flavor can be easily derived from the B_s^0 decay products. The production flavor is determined with help of complex algorithms, so-called flavor tags, which make use of additional information in the event. Finally all information is combined in an unbinned likelihood fit [3]. The mixing related part of the signal likelihood can be written as:

$$\mathcal{L}_{signal,mixing} = \frac{1 \pm D\cos(\Delta m_s t)}{2} \quad (1)$$

where (+)/- correspond to B_s^0 mesons which have (not) mixed between production and decay. D is the so-called dilution, which is introduced by imperfect tagging. The dilution is related to the probability P, that the tag correctly identifies the flavor: $D = 2P - 1$, so a perfect tag has D=1, and a random tag has D=0. If the mixing frequency can be clearly resolved as in the case of the B^0 mixing, we can fit simultaneously for the dilution D and Δm and thus derive both quantities directly from the data itself. This is not true for the B_s^0 system where sofar only lower bounds on the mixing frequency Δm_s have been set. In order to be able set a lower limit or to establish a mixing frequency the dilution has to be known before-hand. A too optimistic estimate of the dilution would potentially result in the exclusion of mixing frequencies to which we are actually not sensitive. The figure of merit for tagging algorithms, which is directly related to the significance for a measurement of the mixing frequency is the so-called tagging performance ϵD^2, where D is the tagging dilution. The efficiency ϵ is the fraction of B candidates to which the flavor tag can be applied ($0 < \epsilon < 1$). The key improvement in the CDF II B_s^0 mixing analysis [4], which pushed the significance up by almost a factor 2 and lead thus to the first direct measurement of the mixing frequency was the development of a new flavor tagging method, the so-called Same-Side (Kaon) Tagging algorithm. First studies using Same-Side Tagging algorithms for the B^+ and the B^0 system have been performed in CDF I already [5]. We present here the analysis of a Same-Side Kaon Tagging algorithm which has been used for the first time in the complex environment of an hadron collider experiments to tag B_s^0 mesons.

II. FLAVOR TAGGING

There are two different classes of flavor tagging, the so-called Opposite-Side Flavor Tag (OST) and the Same-Side Flavor Tag (SST). The OST algorithms exploit the fact that B mesons are mainly produced in pairs with correlated production flavor. Thus, determining the production flavor of the other B in the event allows one to conclude the B production flavor on the signal side. Those tagging algorithms are expected to have small or even negligible dependency on the properties of the signal side. For that reason, it is possible to measure their performance in B^0 and B^+ modes and apply them then to the B_s^0 mixing analysis. Therefore data itself can be used to calibrate OST algorithms as well for the B_s^0 system.
The SST algorithm exploits flavor-charge correlations between the B meson and particles produced in the hadronization process. The principle of Same-Side Tagging is illustrated in Figure 1. In the most simple picture, where only pseudo-scalar mesons are produced directly by the fragmentation process, the following charged stable mesons are expected: a B^0 is produced along with a π^+, a B^+ along with a π^- or a K^-, and a B_s^0 is expected to be produced with a K^+ (therefore this tagging algorithm is called Same-Side Kaon Tag (SSKT) in case of B_s^0). The charge correlation of the B and those fragmentation tracks can be exploited to determine the B production flavor. Additional processes like the formation of neutral particles such as a π^0 or K^* as leading fragmentation particles, or the production of B mesons through the decay of excited B states

lead to more complex scenarios. Therefore we expect different tagging performance for different B species. So, contrary to the OST algorithms, there is no straightforward way to measure the performance of the SSKT algorithm in data without observing clear B_s^0 oscillation signal. We can not transfer the dilution from the B^0 and B^+ to the B_s^0, but have to rely on Monte Carlo simulation to determine the SSKT performance. Detailed understanding of the agreement and potential discrepancies between data and Monte Carlo is mandatory in order to use Monte Carlo based predictions of the SSKT performance for the mixing analysis.
It is much more challenging to develop a SSKT compared to an OST algorithm, but the potential gain is by far larger as well. This is mainly related to the fact that the tracks associated to the leading fragmentation particles are - as the signal B meson itself - in the active detector region, while tracks from the opposite-side B are often not reconstructed. Thus events are either not tagged or their tagging decision is based on false information. Additionally there is a 17 % probability that the opposite-side B has mixed before it decays, thus all opposite-side tagging algorithm have already an intrinsic mis-tag rate of 17 %. This is not the case for the Same-Side Tagging algorithm as we directly tag the production flavor of the signal B. The current OST algorithms in CDF have a combined tagging performance of $\epsilon D^2 \approx 1.5$ %, while we will establish 4.0 % for the SSKT.

III. SAME-SIDE KAON TAGGING ANALYSIS

The analysis of the SS(K)T algorithm has been performed in several steps. First large PYTHIA B^+, B^0 and B_s^0 Monte Carlo samples were generated. A lot of effort is spent into tuning both, the underlying physics processes and detector response. We proved the data and Monte Carlo agreement of the distributions of various tagging related quantities, and their correlations both in the B_s^0 and the high statistics B^+ and B^0 modes. Next we study the performance of several SS(K)T algorithms on the B_s^0 Monte Carlo sample and select and optimize the most promising ones for further studies. The performance of those algorithms is then compared in data and Monte Carlo for the B^0 and B^+ modes. Those modes provide a powerful high statistics cross-check of characteristics of production and fragmentation. After good agreement is achieved, the last and most important step of the analysis is then the evaluation of the systematic uncertainties. Mainly based on our own data we derive ranges for variation of all inputs to our Monte Carlo sample which might have an impact on the SS(K)T performance. Once we are confident that Monte Carlo simulation is properly modeling the B^0 and the B^+ decays and all remaining minor discrepancies are well covered by the systematic uncertainties, we then use the simulation to project the performance on B_s^0 decays.

A. Monte Carlo and Data Samples

This study is performed on a data set which corresponds to an integrated luminosity of 355 pb^{-1}. Large PYTHIA Monte Carlo samples have been generated. While the B meson on the signal side is forced in a specific decay the other one is kept unbiased. The simulated decays are listed in Table I. We studied fully reconstructed modes although statistics is lower than for semileptonic modes. This was motivated by the fact that the main gain in the mixing analysis by using SSKT will come from the fully reconstructed modes due to their better proper decay time resolution. Sample composition and background are harder to handle in case of partial reconstructed modes, which would introduce significant additional systematic uncertainties to the data Monte Carlo comparisons for the B^+ and the B^0 modes. In the following charge conjugated states are implicitly included.

$\bar{b}$-quark	b-quark
$B^+ \to \bar{D}^0\pi^+,\ D^0 \to K^-\pi^+$	$B^- \to D^0\pi^-,\ \bar{D}^0 \to K^+\pi^-$
$B^0 \to D^-\pi^+,\ D^- \to K^+\pi^-\pi^-$	$\bar{B}^0 \to D^+\pi^-,\ D^+ \to K^-\pi^+\pi^+$
$B_s^0 \to D_s^-\pi^+,\ D_s^- \to \phi\pi^-,\ \phi \to K^+K^-$	$\bar{B}_s^0 \to D_s^+\pi^-,\ D_s^- \to \phi\pi^+,\ \phi \to K^+K^-$

TABLE I: Signal side topologies of the PYTHIA Monte Carlo samples.

The PYTHIA [6] event generator has been heavily used and tuned on LEP and Tevatron data and shows overall very good agreement. The PYTHIA code provides various options one can select, to adjust input parameters to recent measurements or to add additional level of details to the event generation. For our analysis it e.g. turned out that next-to-leading order $b\bar{b}$ production mechanisms are not negligible but have

sizeable effects on several kinematic distributions. Although this slowed down the Monte Carlo generation by more than a factor of ten we included them in the production. Various other parameters such as the fragmentation function and the rate of excited B mesons have been tuned based on recent measurements [7] [8]. The (luminosity dependent) effect of multiple interactions in the event has been taken into account by embedding tracks from data into Monte Carlo events.
While the simulation reproduces precisely run-by-run the detector status for most of the detector components the response of the particle identification was not very well reproduced. This was mainly related to the fact time-of-flight (TOF) calibration and reconstruction recently improved significantly. The Same-Side Kaon Tagging algorithm is one of the first analysis which actually use TOF information and definitely the first one which uses TOF and ionization energy loss measurements (dE/dx) in the simulation. The dE/dx and TOF response where simulated accordingly to resolution and efficiency distributions which have been measured on clean particle samples in data.
Table II lists the yields of the data and Monte Carlo samples used in this analysis. The B_s^0 Monte Carlo sample is a factor 65 larger than the corresponding data sample, which allows us to reuse the same sample for validation and optimization of the algorithms as well as for the systematic studies.

mode	MC	data
$B^+ \to D^0\pi^+$	239K	9270
$B^0 \to D^-\pi^+$	142K	8040
$B_s^0 \to D_s^-\pi^+$	34K	560

TABLE II: Data and Monte Carlo yields.

B. Particle Identification

In the case of B_s^0 mesons, selecting kaons in the vicinity is a very good criteria to identify the leading fragmentation track. In the following we will extensively use the CDF particle identification system to identify same-side kaons. The best separation power is provided by the TOF system which has been especially designed to match the momentum range of same-side kaons from the fragmentation of the B_s^0. The difference in time-of-flight from the $p\bar{p}$ interaction point to the TOF system for pions and kaons with a transverse momentum of 1.6(1.3) GeV/c is about 200(300) ps. The $TOF_{measured} - TOF_{expected}$ distribution is used to separate different particle species (Fig. 2). The distribution is well described by a double Gaussian with a core resolution of 100-120 ps which accounts for 85% of the area of the resolution function. Depending on the momentum, 50% - 65% of the tagging track candidates have associated TOF information. dE/dx information is essentially present for all the tagging track candidates and provides an average separation power of about 1.4 σ. Using dE/dx and TOF information we construct a combined likelihood variable to separate kaons from other particle species:

$$\log(LH(PID)) = \log(\frac{PDF_{TOF}(K) * PDF_{dE/dx}(K)}{f_\pi * PDF_{TOF}(\pi) * PDF_{dE/dx}(\pi) + f_p * PDF_{TOF}(p) * PDF_{dE/dx}(p)}),$$

where f_π and f_p are the pion and proton fractions in the background sample ($f_\pi = 0.9$, $f_p = 0.1$).
The simulation reproduces well the $\log(LH(PID))$ distributions in data, both in the high statistics B^0 and B^+ mode as well as in the B_s^0 mode (Fig. 4). Remaining small discrepancies are covered by the systematic uncertainties as will be shown later.

C. Tagging Algorithms

Tracks with a minimum transverse momentum of $p_T \geq 450$ MeV/c, which are likely originated from the same primary interaction as the B meson ($|d_0/\sigma_{d_0}| \leq 4$ & $|\Delta z_0(track, B)| \leq 1.2$ cm) and which are in a cone around the reconstructed B meson ($\Delta R(track, B) = \sqrt{\Delta\phi^2 + \Delta\eta^2} \leq 0.7$) are considered as potential tagging tracks. The multiplicity of tracks in the vicinity of the B meson passing those cuts are shown in Figure 5. In case more than one track in the event fulfills those criteria, and the potential tagging tracks do not all have the same charge, a further selection criteria has to be introduced to actually make a tagging decision. This

affects about 30% of the tagged events. Any difference in tagging algorithms comes from different performance on those events. Various algorithms based on kinematical variables have been studied. Earlier CDF studies performed in Run I [5] preferred an algorithm which selects the track with the smallest transverse momentum relative to the B direction (Fig. 3). Our studies showed significantly better performance for all B types by selecting the track with the largest longitudinal momentum relative to the B direction (Fig. 3), the so-called "max. p_L^{rel}" algorithm. Figure 6 displays the p_L^{rel} distributions in data and Monte Carlo.
A second algorithm specific for the B_s^0 modes has been studied as well. The tagging track candidate with the highest kaon probability is chosen ("max $\log(LH(PID))$" algorithm). This is clearly not optimal for the B^0 case. But rather than optimizing an algorithm for B^0 and B^+, we use those high statistics B modes to test the very same algorithm which shows good performance for the B_s^0.

D. Tagging Performance

Using the unbinned likelihood described in Equation 1, we fit for the dilution of the both algorithms described above in data and Monte Carlo. The B_s^0 production flavor in Monte Carlo has been determined using Monte Carlo truth information. The fit results are shown in Table III. The quoted uncertainties are statistical only. The efficiency is the same for both algorithms as all events with at least one tagging track candidate are tagged by both algorithms. We observe decent data Monte Carlo agreement. The particle ID based algorithm works significantly better for the B_s^0 than the "max p_L^{rel}" algorithm.

		"max p_L^{rel}" algorithm			max "$\log(LH(PID))$" algorithm		
[%]		$B^+ \to D^0\pi^+$	$B^0 \to D^-\pi^+$	$B_s^0 \to D_s^-\pi^+$	$B^+ \to D^0\pi^+$	$B^0 \to D^-\pi^+$	$B_s^0 \to D_s^-\pi^+$
MC	ϵ	55.9 ± 0.1	56.6 ± 0.1	52.1 ± 0.3	55.9 ± 0.1	56.6 ± 0.1	52.1 ± 0.3
	$\mathcal{D}$	25.7 ± 0.3	15.1 ± 0.4	19.0 ± 0.8	24.5 ± 0.3	12.9 ± 0.4	21.8 ± 0.8
data	ϵ	58.4 ± 0.5	57.2 ± 0.6	49.3 ± 2.3	58.4 ± 0.5	57.2 ± 0.6	49.3 ± 2.3
	$\mathcal{D}$	25.9 ± 1.4	13.3 ± 2.9	—	25.4 ± 1.4	14.2 ± 2.9	—

TABLE III: Performance of "max p_L^{rel}" and "max $\log(LH(PID))$" algorithm in data and Monte Carlo.

Different events have different potential dilutions. Figure 7 displays the dependence of the dilution of the "max p_L^{rel}" algorithm on the transverse momentum of the selected tagging track in the simulation. Higher momentum tagging tracks provide higher dilution.
For the "max $\log(LH(PID))$" algorithm the tagging performance has been studied as a function of $\log(LH(PID))$ (Fig. 7). For the B^+ we see high dilution both for more pion like (low $\log(LH(PID))$ values) and more kaon like (high $\log(LH(PID))$ values) tracks. For B^0 the pions are more likely to be correlated to the production flavor, while kaons are mainly uncorrelated to the B production flavor (D=0). This pattern is inverted for the B_s^0, where kaons are good tagging tracks and pions do not carry any information on the production flavor.

In the following we will use p_T or $\log(LH(PID))$ of the selected tagging track to predict on an event-by-event basis the potential dilution. Therefore the likelihood has been modified to:

$$\mathcal{L}_{signal,tagging} = \frac{1 \pm S_D D_{pred} \cos(\Delta m t)}{2}, \tag{2}$$

where D_{pred} is the event-by-event predicted dilution, which has been derived on Monte Carlo. S_D is an overall scale factor to compensate differences between the predicted dilution and the actual asymmetry in the sample. We fit for S_D in the Monte Carlo and B^0 and B^+ data. Again the scale factor S_D can not be determined on the B_s^0 sample before the oscillation is clearly resolved. If the calibration of the predicted dilution has been done properly, S_D has per construction to come out very close to 100% in Monte Carlo, as we derived the shape of the predicted dilutions from the very same sample. Using predicted dilutions from Monte Carlo to fit for S_D in B^+ and B^0 data is a very strong test of the fragmentation model. Scale factors consistent with 100% in data confirm that events with similar p_T or $\log(LH(PID))$ of the selected tagging track have the similar tagging performance in data and Monte Carlo.
Additionally, using predicted dilutions improves the overall tagging performance as more weight is assigned to potentially more valuable events while potential low dilution events are deweighted. The number comparable

to the average dilution is in this case the so-called effective dilution $S_D\sqrt{< D^2_{pred} >}$. The fit results for both algorithms are shown in Table IV. Statistical uncertainties only are quoted. We find scale factors consistent with 100% both in data and Monte Carlo. About 2-5% effective dilution can be gained by exploiting event-by-event predicted dilutions. Again the PID based algorithm works best for B^0_s.

		"max p_L^{rel}" algo			"max $\log(LH(PID))$" algo		
	[%]	$B^+ \to \bar{D}^0\pi^+$	$B^0 \to D^-\pi^+$	$B^0_s \to D^-_s\pi^+$	$B^+ \to \bar{D}^0\pi^+$	$B^0 \to D^-\pi^+$	$B^0_s \to D^-_s\pi^+$
MC	ϵ	55.9 ± 0.1	56.6 ± 0.1	52.1 ± 0.3	55.9 ± 0.1	56.6 ± 0.1	52.1 ± 0.3
	S_D	100.3 ± 0.9	98.0 ± 2.1	100.5 ± 3.3	100.0 ± 0.9	98.5 ± 2.1	98.8 ± 2.5
	$S\sqrt{\langle\mathcal{D}^2\rangle}$	29.0 ± 0.3	17.2 ± 0.4	22.8 ± 0.7	27.5 ± 0.2	17.4 ± 0.4	28.5 ± 0.7
data	ϵ	58.2 ± 0.5	57.1 ± 0.6	49.3 ± 2.3	58.2 ± 0.5	57.1 ± 0.6	49.3 ± 2.3
	S_D	103.6 ± 4.7	110.0 ± 16.0	—	95.1 ± 4.7	104.7 ± 14.4	—
	$S\sqrt{\langle\mathcal{D}^2\rangle}$	30.4 ± 1.3	19.0 ± 2.5	—	25.7 ± 1.3	17.6 ± 2.3	—

TABLE IV: Performance of parameterized "max p_L^{rel}" and "max $\log(LH(PID))$" algorithm in data and Monte Carlo.

E. Systematic Uncertainties

Many sources of systematic uncertainties have been investigated, such as the efficiency and resolution of the PID simulation and reconstruction, the effect of different B^{**} rates on the tagging performance for B^+ and B^0, the relative contribution of different production mechanisms, and the background rate from multiple interactions. All of those show small effects on the final result. The largest contribution to the systematic uncertainties comes from studies related the fragmentation models used in Monte Carlo. This has been addressed in two different studies:

- Particle content around B mesons
  The particle species produced in the vicinity of the B^0_s meson give us some insights into the fragmentation process. A measurement of the content of stable charged particles around the B meson has been performed in a high statistic semileptonic sample [9]. In general the fraction of kaons in data and Monte Carlo agrees for B^0, B^+ and B^0_s, and we confirm a clear excess of kaons around B^0_s mesons in data. This measurement was the first evidence from data that SST might work for B^0_s. Nevertheless, there is a small deficit of kaons in B^0_s data, which is at about 1.5 σ. This could be purely statistical. But as the SSKT algorithm heavily relies on the kaon fraction we assign according systematic variations.
  In addition to the stable charged particles we reconstruct resonances and vector particles such as ϕ, K_s and K^* in data and Monte Carlo. Generally good agreement has been observed, although statistics is fairly low. Systematics are assigned by varying the rate of those particles in simulation within the ranges allowed by the statistical precision.

- Variation within statistics from the data:
  Fragmentation determines the formation of hadrons out of the string. Thus any discrepancies in the fragmentation models used in the simulation compared to data would directly affect the track multiplicity around the B meson, the B momentum and the momenta of the fragmentation tracks. By varying the Monte Carlo sample within the ranges allowed by the statistical uncertainties on the corresponding distributions in B^0_s data, we obtain a model independent estimate of how far the Monte Carlo can be maximally off. This study not only covers uncertainties related to the fragmentation but essentially all other potential sources of systematic uncertainties, as long as they show up in a disagreement between data and Monte Carlo in any of those distributions.

The next step is to check that Monte Carlo distributions including the systematic variations enclose well the data distributions (Fig. 8-9).

Comparing D and S_D on data and Monte Carlo within their statistical and systematic uncertainties we see good agreement. But as this statement can not be made more precise than our uncertainties on the data and Monte Carlo sample itself the combined uncertainties from B^0 and B^+ modes have been added to the final uncertainties which are summarized in Table V and displayed in Figure 10. Additional to the decay modes discussed in previous sections, those plots show the tagging performance for $B^+ \to J/\psi K^+$,

algorithm [%]	value	stat MC	sys MC	data/MC agreement	$\sum$
average dil, max. p_L^{rel}	19.0	$\pm$ 0.8	$^{+1.9}_{-4.4}$	$\pm$ 2.1	$^{+2.9}_{-4.9}$
average dil, max. PID	21.8	$\pm$ 0.8	$^{+2.7}_{-5.2}$	$\pm$ 1.6	$^{+3.2}_{-5.5}$
predicted dil, max. p_L^{rel}	100.5	$\pm$ 3.3	$^{+8.6}_{-17.7}$	$\pm$ 5.5	$^{+10.7}_{-18.8}$
predicted dil, max. PID	98.8	$\pm$ 2.5	$^{+7.1}_{-11.8}$	$\pm$ 7.6	$^{+10.7}_{-14.3}$

TABLE V: Summary of tagging performance and according uncertainties for $B_s^0 \to D_s^- \pi^+$.

$B^+ \to \bar{D}^0 3\pi$, $B^0 \to J/\psi K^{*0}$, $B^0 \to D^- 3\pi$ as well. Those modes have been studied analogously to the $D\pi$ modes to additionally support the good agreement of the tagging performance for B^0 and B^+ in data and Monte Carlo. The only difference between different decay modes of the same B flavor is the B momentum due to different trigger and reconstruction cuts. Otherwise the decay is uncorrelated to the fragmentation process. This supports the conclusion that as well the parameterization and the scale factor derived in this study is applicable to all B_s^0 decay modes used in the mixing analysis.

IV. CONCLUSION

We presented the first analysis of Same-Side Kaon Tagging algorithm of B_s^0 decays, in the complex environment of a hadron collider. One of the key components of this algorithms is the use of the CDF II particle ID system, in particular of the time-of-flight detector which has been added in the upgrade for Run II. Unlike for B^+ and B^0 the tagging algorithm can not be calibrated on data as the fast B_s^0 mixing frequency has not yet been resolved. We therefore had to rely on Monte Carlo simulation and established the ability to properly simulate fragmentation correlations in an hadronic environment. We successfully developed a Same-Side Kaon Tagging algorithm which achieves an effective tagging dilution and tagging performance of:

$$S_D \sqrt{< D^2_{pred} >} = 28.3^{+3.2}_{-4.2}\ \%$$
$$\epsilon S_D^2 < D^2_{pred} >= 4.0^{+0.9}_{-1.2}\ \%$$

This tagger is about 2-3 times more powerful than the opposite-side tagging algorithms used so far. Its application to the B_s^0 mixing analysis resulted in the first direct measurement of the B_s^0 mixing frequency of $17.33^{+0.42}_{-0.21}$(stat.) $\pm$ 0.07 (syst.) ps^{-1} [4]. Within limited statistics, the B_s^0 mixing analysis confirms the proper calibration of the Same-Side Kaon Tagging performance, which can e.g. be seen by an amplitude value consistent with one around the measured mixing frequency (Fig. 11). In combination with the expected large increase in data sample, the Same-Side Kaon Tagging algorithm will play a central role in future precision measurements of Δm_s.

[1] S. Eidelman et *al.*, *The Review of Particle Physics*, Physics Letters B**592**,1 (2004)

[2] CKMfitter Group (J. Charles et *al.*), Eur. Phys. J. C41, 1-131 (2005), [hep-ph/0406184]

[3] CDF Collaboration,
Study of $B_s^0 \to \ell^+ D_s^- X$ Oscillations in the Two-Track Trigger Sample, CDF Public Note 7907,
Updated Study of B_s^0 Oscillations in $B_s^0 \to D_s^-(3)\pi$, CDF Public Note 7941

[4] CDF Collaboration, `www-cdf.fnal.gov/physics/new/bottom/bottom.html`

[5] P. Shpicas et al, for the CDF Collaboration,
Observation of πB Meson Charge-Flavor Correlations and Measurement of Time Dependent $B^0\bar{B}^0$ Mixing
FERMILAB-CONF-96/175-E

[6] T. Sjörstrand, et al, Comp Phys,. Commun. **135**, 238 (2001)

[7] E. Ben-Haim, P. Bambade, P. Roudeau, A. Savoy-Navarro and A. Stocchi,
Extraction of the x-dependence of the non-perturbative QCD b-quark fragmentation distribution component,
Phys. Lett. B **580**, 108 (2004) [arXiv:hep-ph/0302157].

[8] DELPHI Collaboration, *A Study of Excited b-Hadron Sates with the DELPHI Detector at LEP*,
`http://delphiwww.cern.ch/pubxx/conferences/summer05/paper_lp56.ps.gz`

[9] CDF Collaboration,
Study of Charged Particles Species Produced in Association with $\bar{B}^0$, B^- and B_s^0 Mesons in $p\bar{p}$ Collisions at $\sqrt{s}$ = 1.96 TeV, CDF Public Note 8137

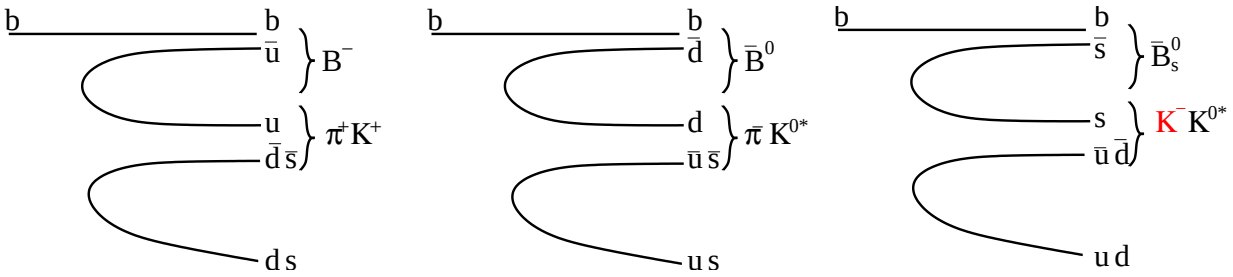

FIG. 1: Illustration of some of the possible particle species produced in the fragmentation of a b quark to a B meson.

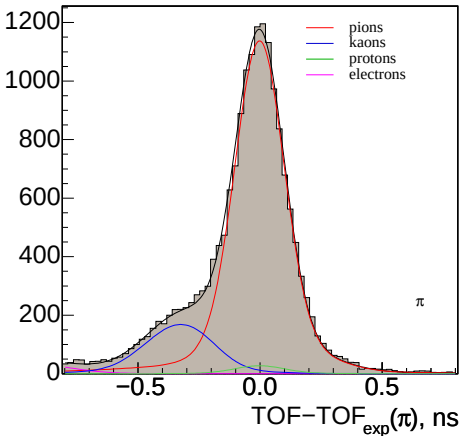

FIG. 2: $TOF_{measured} - TOF_{expected}(\pi)$ distribution for tracks with $1 < p_T < 1.5$ GeV/c in a cone around $B^+ \to \ell^+ \bar{D}^0$ candidates ($\Delta R < 0.7$).

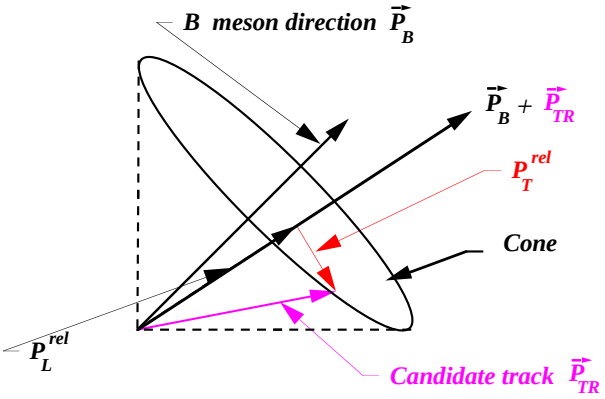

FIG. 3: Illustration of the construction of the quantities p_T^{rel} and p_L^{rel}.

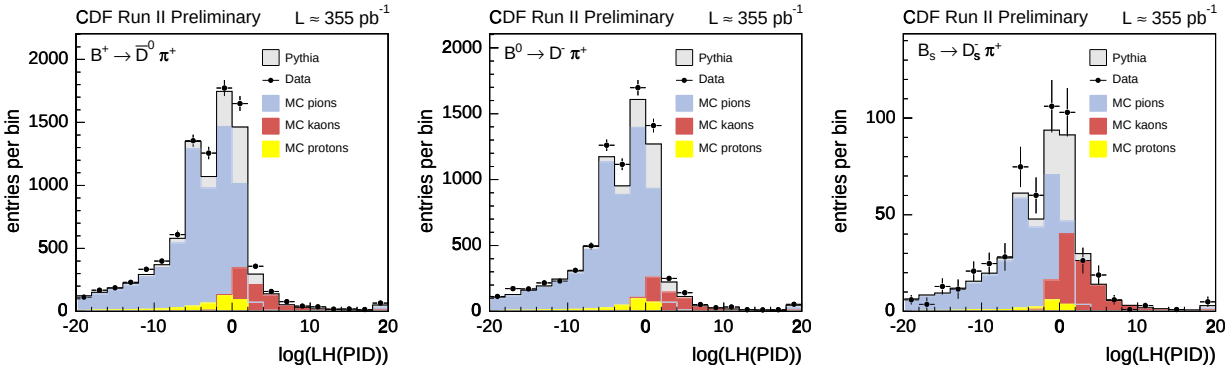

FIG. 4: Comparison of $\log(LH(PID))$ distributions between data and Monte Carlo. Plots are normalized to the number of reconstructed B candidates in data. All discrepancies in those distributions are covered by the systematic variations as shown later.

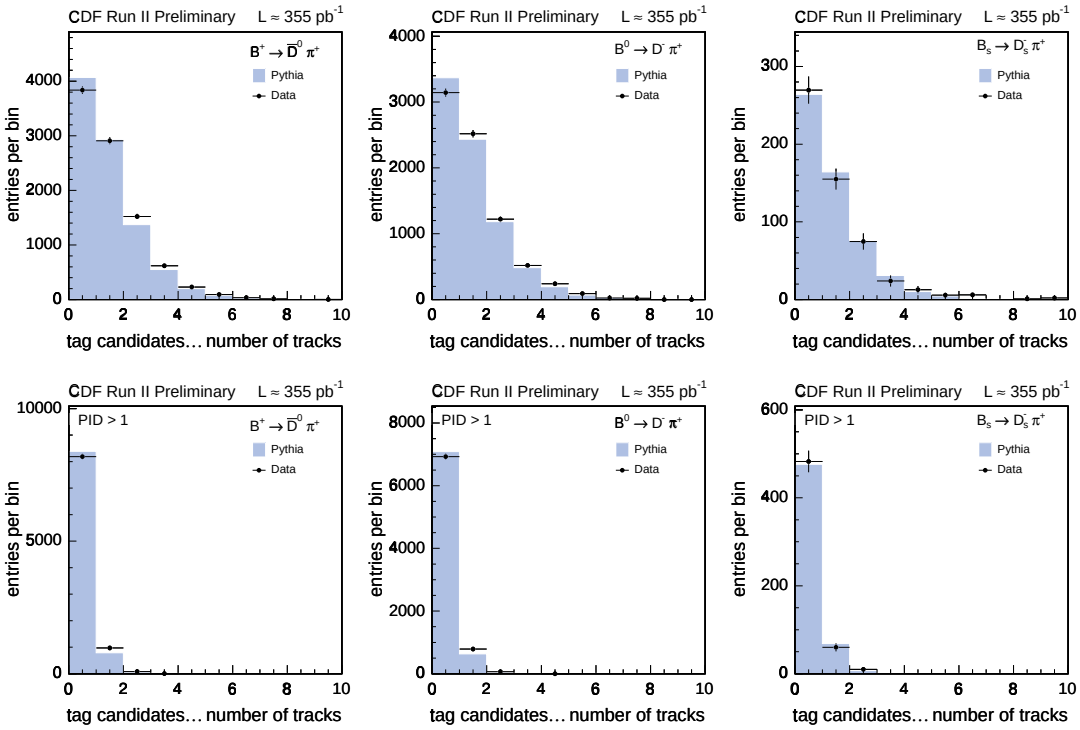

FIG. 5: Data and Monte Carlo comparisons of tagging track multiplicity. In the lower row $\log(LH(PID)) > 1$ is required. Plots are normalized to the number of reconstructed B candidates in data.

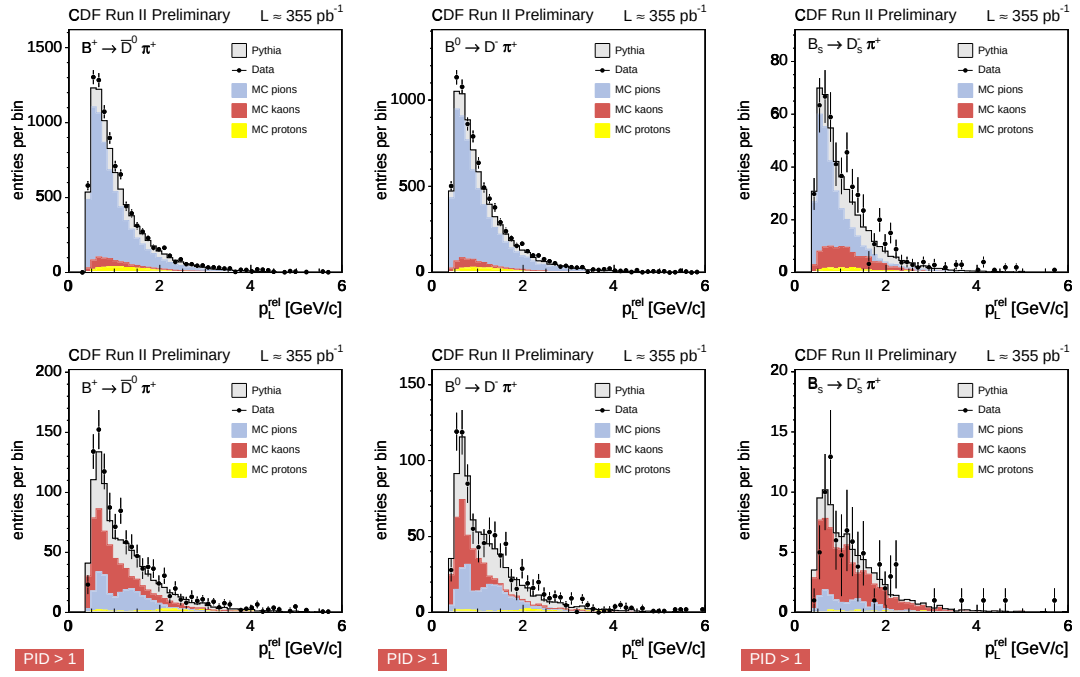

FIG. 6: Comparison of p_L^{rel} distributions of tagging track candidates between data and Monte Carlo. In the lower row $\log(LH(PID)) > 1$ is required. Plots are normalized to the number of reconstructed B candidates in data.

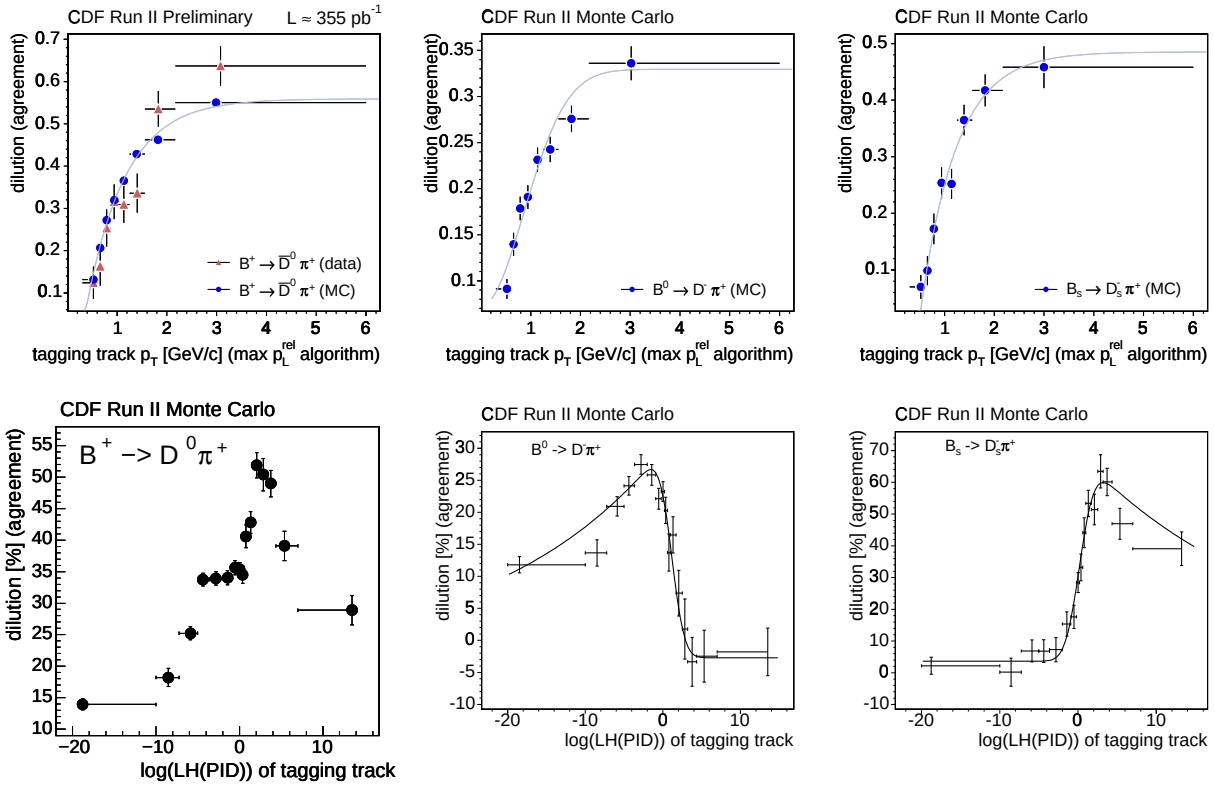

FIG. 7: Dilutions of the "max p_L^{rel}" and "max $\log(LH(PID))$" algorithms as a function of p_T and $\log(LH(PID))$ of the tagging track for cases of agreeing tagging candidate charges in Monte Carlo. For the "max p_L^{rel}" algorithm on B^+ data points are overlaid as well. Light blue/black lines correspond to the event-by-event parameterized dilution function. For the B^+ modes in "max $\log(LH(PID))$" algorithm the event-by-event predicted dilutions are not a parameterized functions but a binned prediction corresponding to the bins shown here.

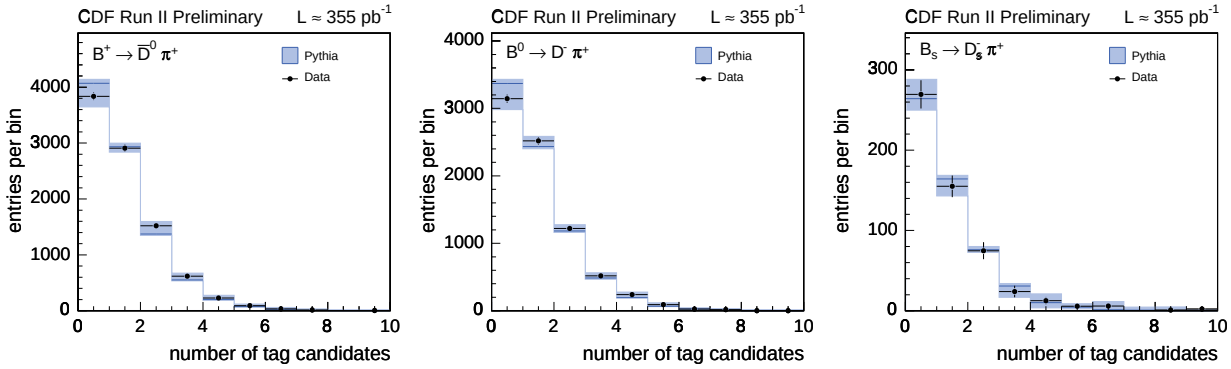

FIG. 8: Data and Monte Carlo comparisons of the multiplicity of tagging track candidates. The blue band corresponds to systematic variations applied to the Monte Carlo sample.

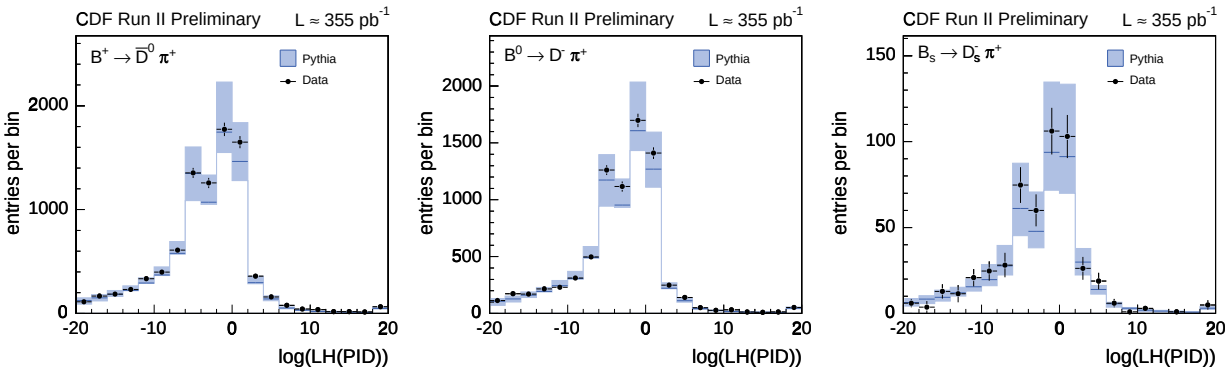

FIG. 9: Comparison of the $\log(LH(PID))$ distributions between data and Monte Carlo. The blue band corresponds to systematic variations applied to the Monte Carlo sample.

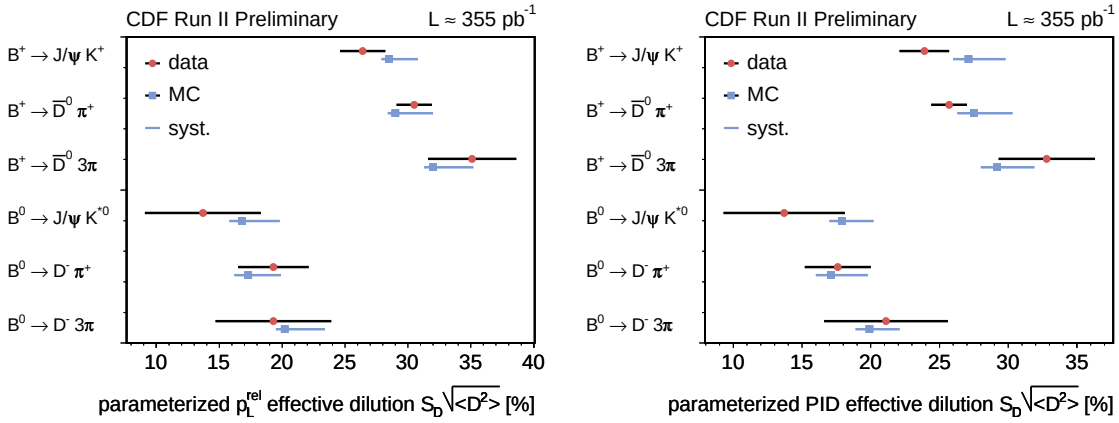

FIG. 10: Data and Monte Carlo comparison of tagging performance.

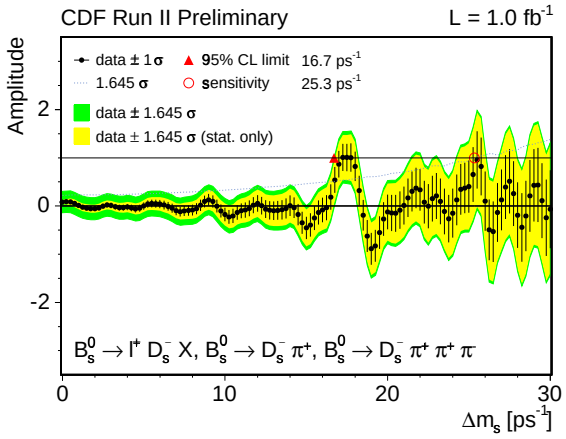

FIG. 11: Amplitude scan for the B_s^0 mixing analysis. An amplitude consistent with 1 around the measured mixing frequency indicates well calibrated tagging algorithms.